Materials Science Forum
ISSN: 1662-9752, Vol. 994, pp 78-87
doi:10.4028/www.scientific.net/MSF.994.78

Submitted: 2019-11-08
Revised: 2019-11-22
Accepted: 2019-11-28
Online: 2020-05-27

The Thermal Effect of Unconventional Cutting Technologies on Steel DIN 1.7102

Pavel Stoklasek[1,a*], Ales Mizera[1,b], Miroslav Manas[1,c] and Martin Ovsik[1,d]

[1]Tomas Bata University in Zlin, nam. T. G. Masaryka 5555, 760 01, Zlin, Czech Republic

[a*]pstoklasek@utb.cz, [b]mizera@utb.cz, [c]manas@utb.cz, [d]ovsik@utb.cz

Keywords: nanohardness, depth sensing indentation, mechanical properties, laser cutting, plasma cutting, wire electrical discharge machining, waterjet cutting, heat-affected zone

Abstract. New technologies known as unconventional technologies make it possible to cut complex shapes at high speed and with relatively high precision. In many cases, especially in the case of thin sheet, created parts produced do not require any further treatment by post-machining. Knowledge of the accompanying phenomena, such as the heat-affected zone (HAZ) or the surface quality of the cutting edge, is necessary, for example, to assess further machining of material in these areas (e.g. drilling and reaming holes or finishing operations on the cutting edge). In this study, the thermal effect of four unconventional cutting technologies – laser, plasma, wire electrical discharge machining (wire EDM) and waterjet cutting on the cut surface of steel sheets is investigated. Steel 1.7102 (DIN 54SiCr6) was chosen for purpose of this study. The width of the HAZ and the nanohardness beneath the cut surface were analyzed.

Introduction

In industrial production, cutting of a material, especially sheets or plates, is often already included in material preparation operations. A large number of these operations in the manufacturing processes force suppliers to reduce costs and increase productivity while maintaining the required accuracy and quality of the preforms or of the finished products.

Mechanical cutting methods, both chip and chipless, are well known and widely described. However, these methods are limited only to straight cuts, which excludes their applicability, in particular for complicated shapes. Some materials, especially those with worse machinability, cannot be cut at all with these technologies. These limiting factors have led to the development of so-called unconventional methods suitable for machining and cutting materials.

Unconventional cutting methods use physical, chemical or mechanical processes or their combined effects to remove material from the cutting kerf. These methods include, for example, laser, plasma and waterjet cutting or wire EDM. By using unconventional methods, it is possible to cut 2D and 3D shapes, increase accuracy and accelerate production. [1,2]

Most unconventional metal cutting methods are based on local melting of the material and its removal from the cutting kerf. The HAZ is formed around the cutting edge due to the thermal effect of the laser or plasma beam. HAZ is described as a non-molten region of metal near the cutting edge in which the material properties or internal structure have changed (compared to the non-thermally affected base material). The formation of HAZ is usually an undesirable side effect of unconventional cutting methods. The term HAZ is also widely used in the welding, where it defines an area close to the weld with other chemical and mechanical properties than the weld material and the base material. [3-7]

The heat-affected area usually consists of multiple bands. The widest band (the band with the most significant thermal effect of the cutting beam) is called the main band. There are very significant differences in properties compared to the base material (e.g. increase in hardness, decrease in chemical or corrosion resistance or worse machinability). The main zone is followed by a transition zone in which the differences between the main zone and the base material are balanced. The width of the HAZ bands for different materials varies depending on the chemical composition, material thickness, intensity and concentration of the thermal effect used in the cutting process. [8-12]

Appropriate process parameter settings also have a significant influence on the width of the HAZ. Cutting methods that operate at high temperatures and slow feed speeds result in a wide HAZ. Vice versa, methods that operate at lower temperatures and high feed speeds result in narrow HAZ. [13-15]

Experimental Methods

The examined material. The steel 1.7102 is a medium-carbon spring steel with difficult weldability commonly used for the production of highly stressed automotive and railway suspension springs, high-dynamic loaded pars like valve springs, flat parts requiring wear resistance (working parts of construction and agricultural machinery) or long blades such as swords, machetes and combat knives. The steel 1.7102 is often shipped in the annealed state, is not straightened and does not exhibit corrosion resistance, including atmospheric resistance. Thermally and mechanically treated sheets have high strength, hardness and abrasion resistance, but machinability, workability and weldability is low. The chemical composition of the steel 1.7102 is reported in Table 1. The ferritic-pearlitic microstructure of base material is shown in Fig. 1. The indentation hardness of the base material was measured at 10 locations of the specimen. The average value of the indentation hardness was 296 ± 5 HV.

Table 1. Chemical composition of steel 1.7102

C [max. %]	**Mn** [max. %]	**Si** [max. %]	**P** [max. %]	**S** [max. %]	**Cr** [max. %]	**Ni** [max. %]	**Cu** [max. %]
0,60	0,80	1,60	0,035	0,035	0,70	0,5	0,30

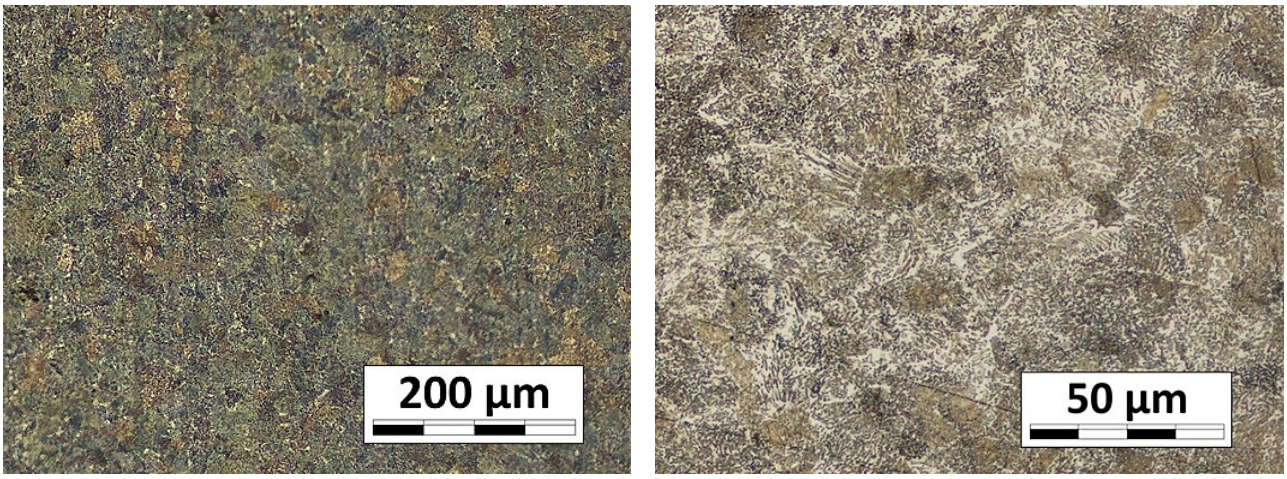

Fig. 1. The structure of the base material – steel 1.7102

The test specimen. The width of the HAZ and the quality of the cutting surface is primarily determined by the selection of optimal process parameters for the particular type and thickness of the material. The test specimens were manufactured under commonly used process parameters based on the recommendations of the cutting technology supplier. These recommendations are made empirically for specific material and its thickness and are implemented in programs that create a CNC cutting program. The subject of this work is not to investigate the influence of variable process parameters on the quality of cut or width of HAZ, but the influence of commonly used parameters in industrial production.

All test specimens were made from commercially available material 1.7102 steel sheets with a thickness of 15 mm. The surface of the sheets was not specially treated and was not cleaned or degreased before cutting. The dimensions of the test specimen were 25 x 25 mm.

The test specimens for determining the thermal effect of the laser were created using a CO2 laser on the Trumpf TruLaser 3030. The output laser power was 3200 W and cutting speed was 1100 mm/min.

The test specimens to determine the thermal effect of plasma cutting were produced on a Kjellberg CNC cutting machine using a HiFocus 80i plasma inverter. The output current was 80 A and cutting speed was 1200 mm/min.

Test specimens for determining the thermal influence of wire EDM were made on a FANUC ROBOCUT α-CiB. The diameter of the brass wire used was 0.25 mm and the wire feed rate was 6 mm/min. Deionized distilled water was used as the dielectric liquid.

Test specimens to determine the effect of waterjet cutting were manufactured on a Flow WaterJet Mach 4020c. An abrasive with a grain size of 150 – 300 μm was used. The water pressure was 380 MPa, the feed rate was 60 mm/min and the abrasive flow rate was 0.45 kg/min. It has been proven that waterjet cutting does not have any thermal effects on the material during production. However, this technology is part of this work to compare and verify that there are no slight changes in hardness near the cut area.

To achieve excellent DSI hardness analysis results it is essential to prepare an optimal specimen surface through a series of processes: cutting, mounting, grinding and polishing. However, it was first necessary to create a cut on the test specimens that would enable measurement of the mechanical properties of the HAZ and metallographic analysis. All specimens were cut with a diamond cutting disc on a metallographic cutter at half its length. The blade speed was set to 1800 rpm and the blade feed was set to 16 mm/min. The cutting edge was intensively cooled to prevent any additional thermal influence on the cutting area. The grain direction in the material was not taken into account when cutting the specimen. However, care was taken to ensure that the point of entry of the beam into the material always lies outside the cut. The described procedure of the specimen preparation is shown in Fig. 2

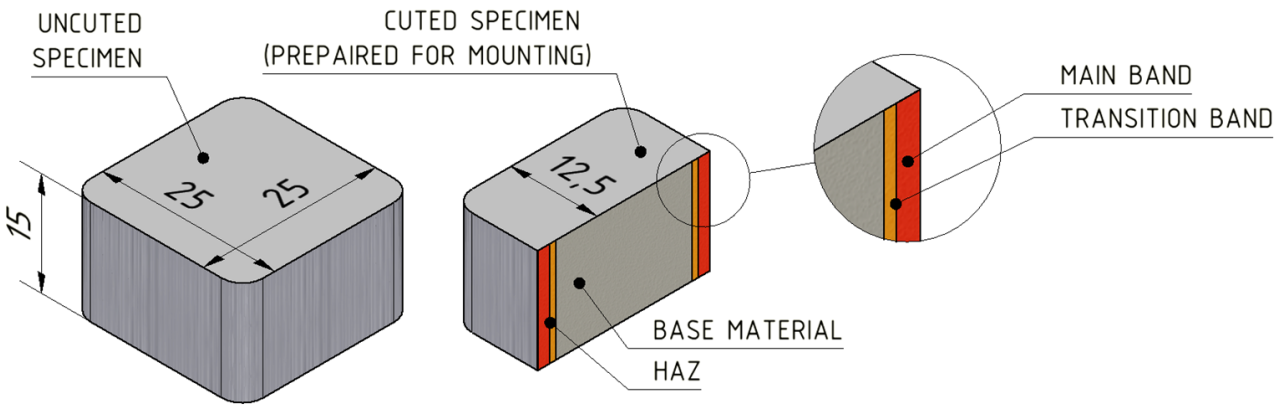

Fig. 2. The specimen preparation

The hardness measurement. The hardness in the HAZ was measured by DSI method according to EN ISO 14577-1 on a TTX-NHT2 Nanoindentation Tester (Anton Paar, Switzerland). Three-sided pyramidal Berkovich tip was used as indenter. The optional parameters of the instrumented indentation test have been set with respect to the recommendations given in EN ISO 14577-1: maximum applied load 500 mN, endurance at maximum load 15 s and loading and unloading speed of indentation 1 N/min.

A matrix measurement was used to determine the hardness and width of the HAZ. The measurement matrix contained a total of 39 positions in one row, extending to a depth of 5 mm from the cutting edge. The distance between two adjacent indentations was set to 50 μm up to a depth of 1.5 mm from the cutting edge. From this distance, the next step between two adjacent indentations was set to 500 μm up to a depth of 5 mm.

The HAZ hardness measurements were performed at six different locations of the specimen – both sides at the top 15 % of the sheet thickness from the top surface, at 50 % of the sheet thickness and

85 % of the sheet thickness. The principle of hardness measurement is shown in Fig. 3. Multiple HAZ hardness measurements on one specimen help to reduce the inhomogeneity of the internal structure of the material. The measured data were evaluated by the Oliver & Pharr method. The main results of the indentation test were the indentation hardness and the maximum indentation depth.

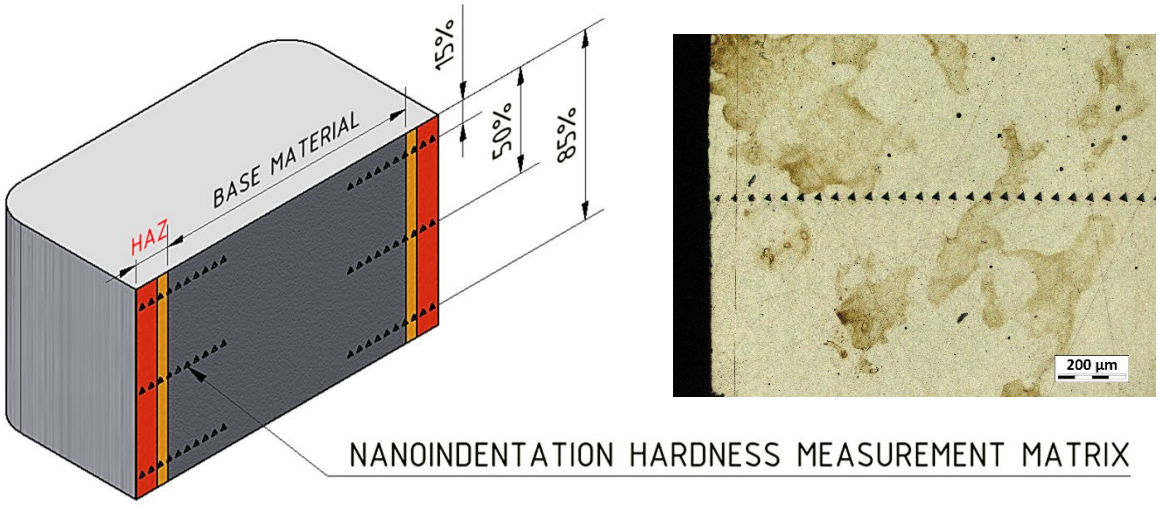

Fig. 3. The principle of nanohardness measurement

During grinding of some test specimens, the surface for hardness measurement was undercut due to different hardnesses of resin, HAZ material and base material. The undercut on the metallography sample is shown in Fig. 4. Because of this phenomenon, each measurement matrix included an operation to determine the actual surface height between indentations.

Determining initial indenter height is one of the most important parameters of nanohardness measurement - it is a theoretical point, where the indenter contacts the surface of the test specimen.

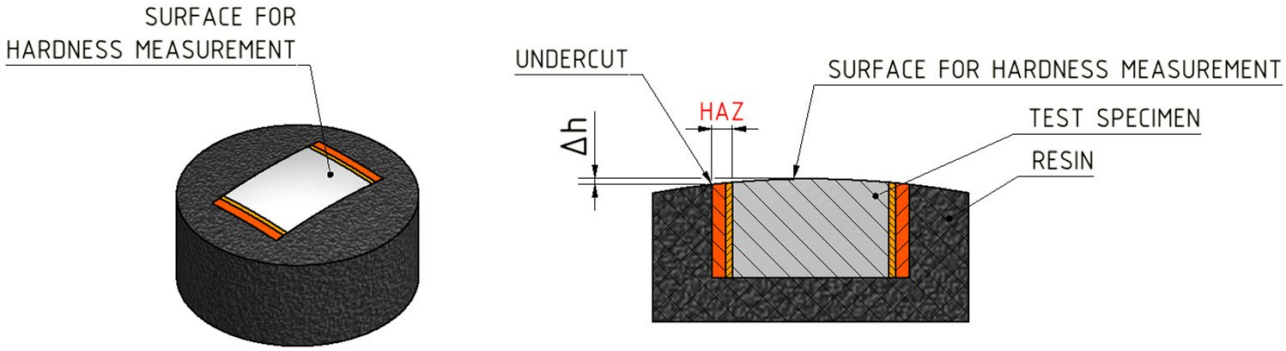

Fig. 4. The undercut on the metallography sample

During the measurement, the initial position of the specimen surface is normally determined by penetrating the indenter into the surface at the lowest possible load of the tester (in units of µN). The next measured indentation depth is then adjusted by this value. The initial indenter height determination is performed near the hardness measurement area. An example of measurement with this element is shown in Fig. 5. The use of initial indenter height determination in the measurement matrix significantly accelerated the length of individual measurements and reduced the risk of measurement errors.

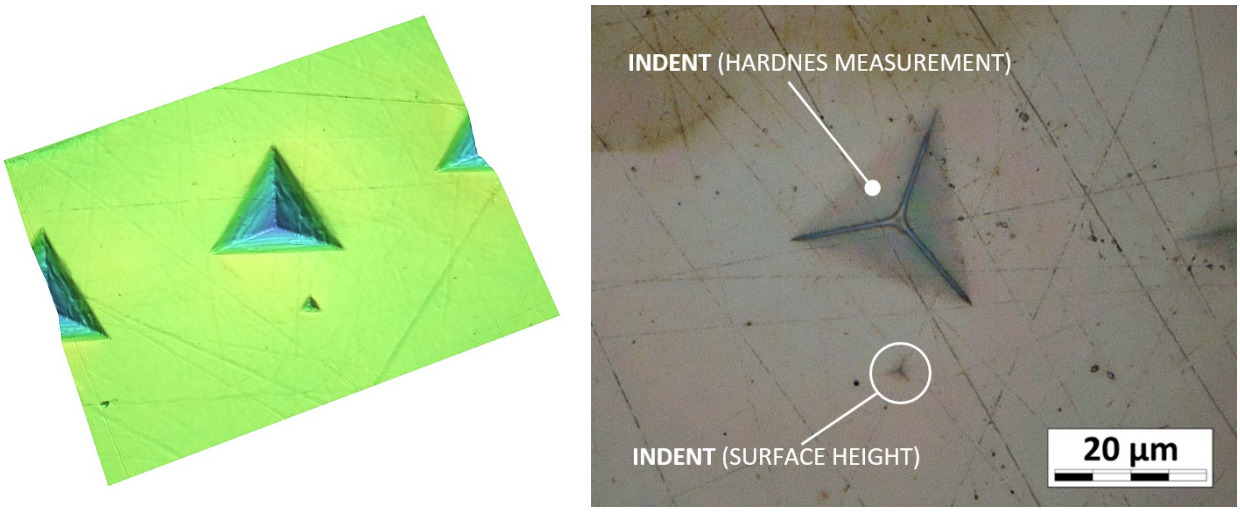

Fig. 5. Detail of hardness measurement matrix with surface height indentation

The hardness measurements of test specimens produced by all selected material cutting methods is shown in Fig. 6. The results show different thermal effects of selected technologies on the cutting edge. The higher thermal effect of plasma cutting causes a wider HAZ compared to laser cutting. There are also differences in the highest measured hardness in the main band of HAZ. It was shown that the maximum hardness is observed near the cut surface and gradually decreases until it reaches the hardness of the base material. The highest hardness achieved in HAZ by plasma cutting is 950 HV, the highest hardness achieved by laser cutting is 850 HV. It is also apparent that waterjet cutting and wire EDM does not produce a HAZ with a measurable change of hardness. However, metallographic analysis showed that during laser, plasma and wire EDM cutting a thin layer with a different structure from the base material was formed near the cutting edge. The hardness of this layer was not measurable by the set parameters due to its width and location on the cutting edge of the specimen.

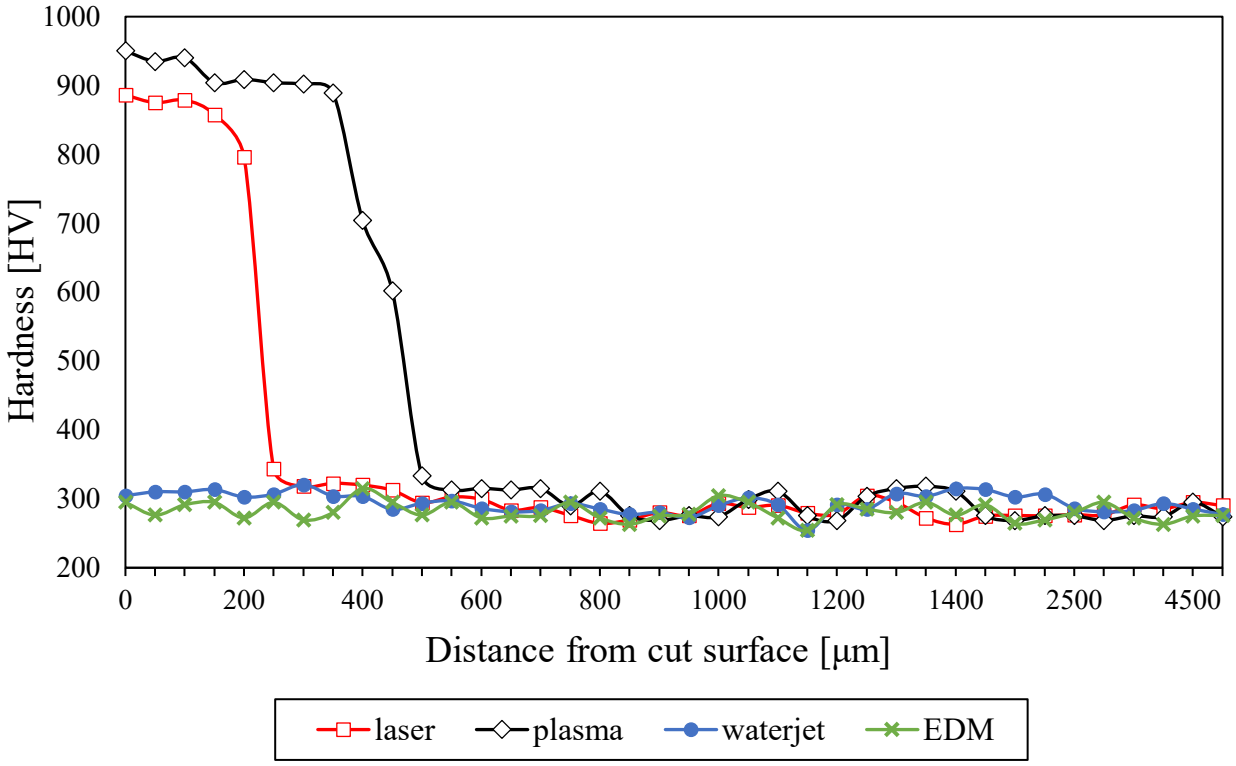

Fig. 6. The influence of different cutting methods on the HAZ nanohardness

Optical analysis. Optical analysis of the HAZ width and internal structure of etched test specimens was performed on a 3D laser scanning microscope (Keyence, Japan). A Nital (5% nitric acid) was used as etching agent. The optical analysis results of all selected cutting methods is shown in Fig. 7

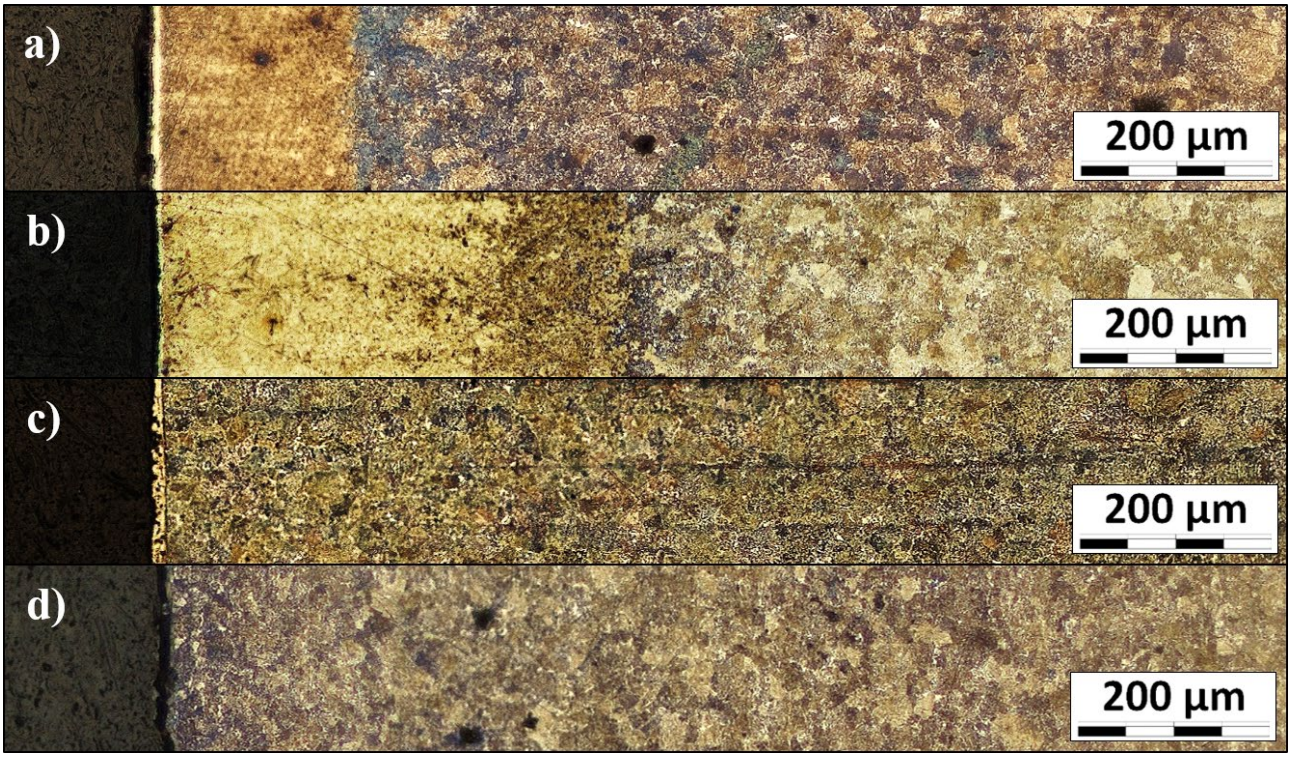

Fig. 7. The influence of different cutting methods on the HAZ width
a) laser cutting b) plasma cutting c) wire EDM cutting d) waterjet cutting

Optical analysis of the laser-cut specimen revealed the HAZ with a total width of 210 µm. In total, this HAZ area consists of three bands. The first band is about 12 µm wide and its martensitic structure is similar to the so-called white layer that occurs when cutting EDM. This band is followed by the main HAZ band. Its structure consists of a needle-like martensitic structure. The main HAZ band is followed by a very narrow 45 µm wide transition area, in which almost immediate change to the ferritic-pearlitic structure of the base material occurs. A comparison of the measured HAZ band widths and the estimated hardness measurements is shown in Table 2.

Table 2. Width of HAZ bands during laser cutting

	Width estimation from hardness test [µm]	**Average of measured values from optical analysis** [µm]
white layer width	not identified	12
main band width	200	213
transition band width	50	45
HAZ width	250	250

When cutting the specimen with a plasma beam, the HAZ of approximately 490 microns was formed near the cutting edge. Similar to a laser-cut specimen, the HAZ consists of three bands. The first band is about 7 microns wide and consists of a martensitic structure. This band is followed by the main HAZ band, which is approximately 370 µm wide. The structure of this band consists of a needle-like martensitic structure. The HAZ main zone is followed by a transition zone approximately 110 µm wide. In this zone, the martensitic structure gradually changes to the ferritic-pearlitic structure

of the base material. A comparison of the measured HAZ band widths and the estimated hardness measurements is shown in Table 3.

Table 3. Width of HAZ bands during plasma cutting

	Width estimation from hardness test [μm]	**Average of measured values from optical analysis** [μm]
white layer width	not identified	7
main band width	350	380
transition band width	150	110
HAZ width	500	490

The optical analysis of test specimens produced by the thermal cutting methods showed the presence of minor surface defects at the cutting edge. When the laser or plasma beam leaves the cutting area, the cutting edge is rapidly cooled to ambient temperature. Due to the rapid cooling of the cutting edge, internal stresses have occurred in the HAZ. This resulted in the formation of cracks and their further spread along the grain boundaries. Areas with this type of damage have deteriorated mechanical properties and lower corrosion resistance. Crack found in the HAZ of the specimen during plasma cutting is shown in Fig. 8

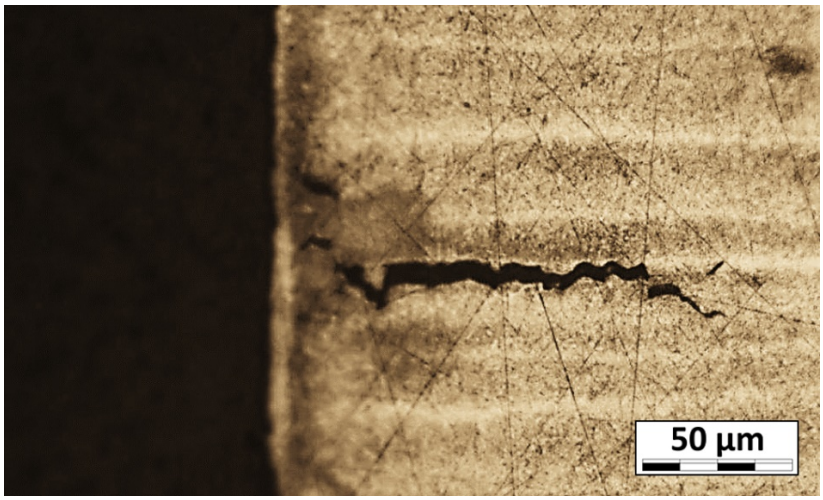

Fig. 8. A crack near the cutting edge on the plasma-cut specimen

The hardness test results of the wire EDM-cut specimen showed no changes to indicate the presence of the HAZ. Optical analysis, however, confirmed the formation of a very narrow layer, which is described in literature [16-18] as the so-called white layer. This 9 – 10 microns wide layer has a martensitic structure and is stable over the entire length of the cut. Beyond this layer, optical analysis revealed no transition zone - an immediate change to the ferritic-pearlitic structure of the base material follows. A comparison of the measured HAZ band widths and the estimated hardness measurements is shown in Table 4.

Table 4. Width of HAZ bands during wire EDM cutting

	Width estimation from hardness test [μm]	**Average of measured values from optical analysis** [μm]
HAZ width	not identified	10

The optical analysis of water jet cut specimens showed no HAZ or other optically identifiable layer with a different structure than the base material. A comparison of all optical analysis results is shown in Fig. 9.

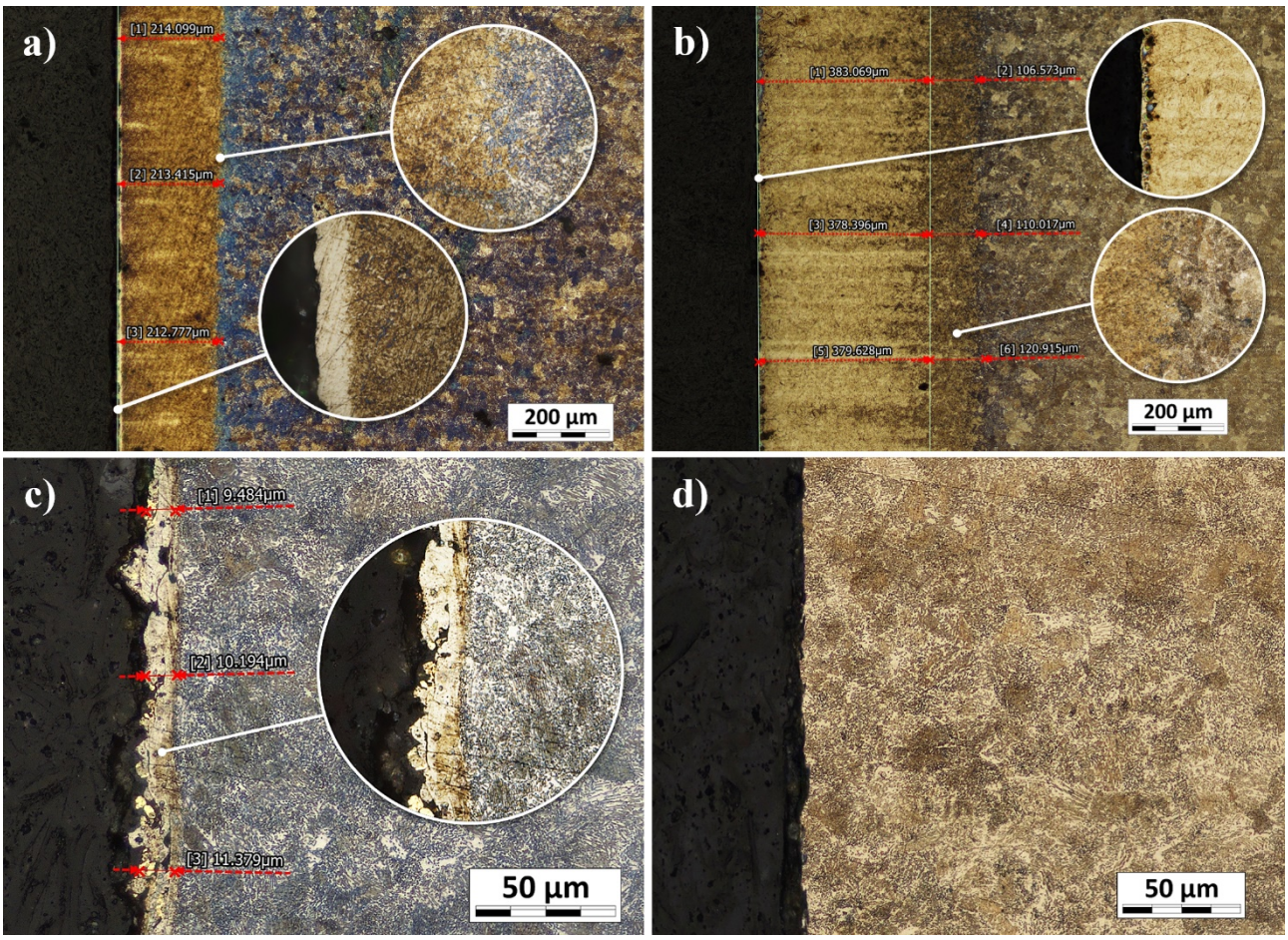

Fig. 9. Optical analysis of different cutting methods
a) laser cutting b) plasma cutting c) wire EDM cutting d) waterjet cutting

Conclusions

The aim of this work was to determine the influence of selected unconventional cutting methods on the change of mechanical properties of steel 1.7102 near the cutting edge. When cutting steel 1.7102 by laser and plasma, the highest measured indentation hardness in HAZ reached 890 - 950 HV. The carbon content, the proportion of residual austenite and its distribution in the thermally unaffected base material have the most significant influence on the width and hardness of the HAZ.

Process parameters of production machines also have a significant influence on HAZ width. Cutting methods operating at higher temperatures and lower speeds create a wider HAZ. The measurements showed that the thermal effect of the plasma beam is significantly higher than the thermal effect of the laser beam. This finding is supported by both indentation hardness and metallographic analysis.

The results obtained from DSI nanohardness measurements provide a very accurate estimate of the HAZ width, which can only be detected by metallographic and optical methods in industrial production.

Conflict of Interests

The authors declare that there is no conflict of interests regarding the publication of this paper.

Acknowledgment

This paper is supported by the Ministry of Education, Youth and Sports of the Czech Republic within the National Sustainability Programme project No. LO1303 (MSMT-7778/2014) and also by the European Regional Development Fund under the project CEBIA-Tech No. CZ.1.05/2.1.00/03.0089.

References

[1] M. Ruppenthal, C. Burnham, Exploring complementary cutting methods. Comparing capabilities of laser, plasma, EDM to waterjet technology, Fabricator, (2001), 46-47.

[2] E. Herghelegiu, C. Schnakovszky, M. Radovanovic, C. I. Raveica, Comparative study on the dimensional accuracy and surface quality of plates cut through unconventional methods, In Proceedings of the International Conference Modern Technologies, Quality and Innovation-ModTech (2012), 24-26

[3] P. Mohyla, Investigation of heat affected zone of steel P92 using the thermal cycle simulator. World Acad Sci Eng Technol, International Journal of Chemical, Molecular, Nuclear, Materials and Metallurgical Engineering 11, no. 6 (2017) 460-463.

[4] I. Miraoui, I., M. Boujelbene, M. Zaied, High-power laser cutting of steel plates: Heat affected zone analysis, Advances in Materials Science and Engineering, 2016, (2016), 1-8

[5] Y. Yang, B. Yan, J. Li, J. Wang, The effect of large heat input on the microstructure and corrosion behaviour of simulated heat affected zone in 2205 duplex stainless steel. Corros. Sci, 53 (2011), 3756-3763.

[6] I. Miraoui, M Boujelbene, M Zaied, High-power laser cutting of steel plates: heat affected zone analysis. ADV MATER SCI ENG, 2016, 1-8.

[7] J. Grum, D. Zuljan, Analysis of heat effects in laser cutting of steels, JMEP, 1996, (5) 526–537.

[8] A. Lazarevic, D. Lazarevic, Investigations of material hardness and structural changes in the heat-affected zone during plasma cutting. WELD WORLD, 2017. 61, 1069-1075.

[9] M. S. Węglowski, T Pfeifer, Influence of cutting technology on properties of the cut edges. INT J ADV MANUF TECH, 2014, (38).

[10] Y. H. Çelik, Investigating the effects of cutting parameters on materials cut in CNC plasma. MATER MANUF PROCESS, 2013, (28), 1053-1060.

[11] M. S. Alsoufi, Experimental study of surface roughness and micro-hardness obtained by cutting carbon steel with abrasive waterjet and laser beam technologies. AJMIE, 2016, (4), 173-181.

[12] N. Jebbari, M. M. Jebari, F. Saadallah, A. Tarrats, R. Bennaceur, and J. P. Longuemard, Themal affected zone obtained in machining steel XC42 by high-power CO2 laser, OPT LASER TECHNOL, 2008 (40,) 864–873.

[13] I. Miraoui, E. Elimi, M. Boujelbene, and E. Bayraktar, Analysis of roughness and microstructure for high-power laser cutting of stainless steel, Adv. Sci. Lett., 2013 (19), 483–486,

[14] D. Patidar, R. S. Rana, The effect of CO2 laser cutting parameter on Mechanical & Microstructural characteristics of high strength steel-a review. MATER TODAY, 2018, (5), 17753-17762.

[15] I. Miraoui, E. Bayraktar, and E. Bayraktar, Effects of laser cutting main parameters on microhardness and microstructure changes of stainless steel, Adv. Mat. Res., 2013 (664), 811–816.

[16] Y. Yildiz, Prediction of white layer thickness and material removal rate in electrical discharge machining by thermal analyses, J. Manuf. Process, 23 (2016), 47-53.

[17] B. Ekmekci, Residual Stresses and White Layer in Electric Discharge Machining (EDM), Applied Surface Science. 253 (2007), 9234-9240.

[18] M. Shabgard, S.N.B. Oliaei, M. Seyedzavvar, A. Najadebrahimi, Experimental investigation and 3D finite element prediction of the white layer thickness, heat affected zone, and surface roughness in EDM process. JMST, 25 (12), 3173-3183.